Yaxu Zheng, Fuming Wang*, Changrong Li, Zhanbing Yang and Yutian He

Effects of B on the Hot Ductility of Fe-36Ni Invar Alloy

https://doi.org/10.1515/htmp-2018-0076
Received May 01, 2018; accepted September 20, 2018

Abstract: This work conducted systematic studies on the effect of B on the hot ductility behavior of Fe-36Ni alloy over the temperature range of 900–1,200 °C by use of Gleeble-3500 thermal simulator, Thermo-Calc software, transmission electron microscopy and secondary ion mass spectroscopy. The influencing factors and mechanisms are also discussed in the present work. Results show that all the values of area reduction of the investigated alloy samples are below 60 % in the temperature range of 900–1,000 °C, indicating the poor hot ductility of the investigated alloys in this temperature range. When the grain boundary sliding occurs during the hot tensile processes, the fine secondary phase particles at grain boundaries prevent the occurrence of dynamic recrystallization and promote the nucleation and propagation of cracking simultaneously, resulting in the poor hot ductility of the investigated alloys in this temperature range. In the B bearing alloy, the segregation of B atoms around austenite grain boundaries promotes the solute dragging effects at grain boundaries and strongly inhibits the occurrence of dynamic recrystallization, which increases the brittle temperature to 1,000 °C. When the temperature exceeds 1,050 °C, the occurrence of dynamic recrystallization improves the hot ductility significantly. However, the coarsening of recrystallized grains and the formation of inter dendritic cracks decrease the hot ductility of the alloy gradually when the temperature increases from 1,100 °C to 1,200 °C.

***Corresponding author: Fuming Wang,** School of Metallurgical and Ecological Engineering, University of Science and Technology Beijing, Beijing 100083, China; State Key Laboratory of Advanced Metallurgy, University of Science and Technology Beijing, Beijing 100083, China, E-mail: wangfuming@metall.ustb.edu.cn
Yaxu Zheng, School of Metallurgical and Ecological Engineering, University of Science and Technology Beijing, Beijing 100083, China; State Key Laboratory of Advanced Metallurgy, University of Science and Technology Beijing, Beijing 100083, China
Changrong Li, School of Materials Science and Engineering, University of Science and Technology Beijing, Beijing 100083, China
Zhanbing Yang, Yutian He, School of Metallurgical and Ecological Engineering, University of Science and Technology Beijing, Beijing 100083, China; State Key Laboratory of Advanced Metallurgy, University of Science and Technology Beijing, Beijing 100083, China

Keywords: Fe-36Ni alloy, hot ductility, secondary phase particles, grain boundary segregation, dynamic recrystallization

Introduction

Fe-36Ni invar alloy is widely used in liquefied natural gas containers owing to its uniquely low coefficient of thermal expansion below the Curie point [1]. However, cracking frequently occurs during the deformation of Fe-36Ni alloy at high temperatures due to the poor hot ductility of austenite [1–3]. Hence, it is necessary to study the hot ductility behavior of Fe-36Ni alloy.

Many researchers [4, 5] reported that the hot ductility of Fe-36Ni alloy is comprehensively influenced by the segregation of elements around grain boundaries, distribution of secondary phase particles and dynamic recrystallization. The segregation of sulfur atoms to grain boundaries deteriorates hot ductility of Fe-36Ni alloy, since it decreases grain boundary cohesion and promotes grain boundary sliding significantly [6]. Hence, the inhibition of segregation of sulfur atoms to grain boundaries effectively improves the hot ductility of Fe-36Ni alloy. Many previous researches reported that boron also tends to segregate to grain boundaries. The diffusion coefficient of boron is larger than that of sulfur [7], which effectively inhibits the segregation of sulfur to grain boundaries. However, the effect of boron on the mechanical properties of steels at high temperatures is complex [8]. Many previous researches [9–11] reported that the addition of boron in carbon steels improved the hot ductility in ferrite and austenite temperature region and single austenite temperature region simultaneously by the acceleration of dynamic recrystallization and inhibition of ferrite transformation. However, the formation of fine Boron nitride (BN) precipitates on grain boundaries strongly deteriorates the hot ductility in the lower austenite temperature region [12].

Although many investigations have been conducted to study the mechanisms of boron on hot ductility of steels, there are few reports about the effect of boron on hot ductility of Fe-36Ni alloy. Only Y. Yu [13] reported that the addition of 0.01 % boron improved the ductility of Fe-36Ni alloy in the temperature range of 850–1,000 °C.

The area reduction was above 80 % and the fracture mode was ductile. However, the Fe-36Ni alloy investigated by Y. Yu contained 0.14 % Mn and 0.002 % S. It was reported [14] that when the actual Mn:S ratio is higher than the critical Mn:S ratio (Mn:S)c, the free sulfur is prevented to segregate to grain boundaries due to the formation of MnS. The formula for calculating the (Mn:S)c is as follows:

$$(\mathrm{Mn:S})\mathrm{c} = 1.345\,\mathrm{S}^{-0.7934}. \quad (1)$$

The values of (Mn:S)c was 186.25 for alloys Y. Yu investigated, which was larger than the actual values of (Mn:S), 70. Therefore, the Mn content in the investigated alloys was not high enough to combine with all the free sulfur atoms. The segregation of sulfur to grain boundaries was detrimental to the hot ductility. With addition of 0.01 % boron, the segregation of boron to grain boundaries inhibited the segregation of sulfur. Therefore, the hot ductility was improved.

In this paper, the actual value of (Mn:S) in investigated Fe-36Ni alloy is higher than the critical value. The Mn fixes the free sulfur atoms. Under this condition, the segregation behavior of boron and precipitation behavior of boron containing particles around grain boundaries in Fe-36Ni alloy have been studied. The present work aims to study the effect of low boron content (0.0021 %) on the hot ductility of Fe-36Ni alloy. The relationships among the boron segregation, precipitates, dynamic recrystallization and the hot ductility behavior of Fe-36Ni alloy were also discussed.

Materials and methods

The 21 kg vacuum induction furnace was used to produce the experimental Fe-36Ni alloys. The ingots were heated to 1,200 °C and held for 2 h, and then they were forged into bars with a diameter of 15 mm. The steel bars were air cooled to room temperature after forging. The chemical compositions of the experimental materials are shown in Table 1. Cylindrical tensile specimens with a diameter of 10 mm and a length of 121.5 mm were machined from the as-wrought bars along their longitudinal direction.

The Gleeble-3500 thermal simulator testing machine was used to conduct the hot tensile testing. The temperature range of tensile testing was from 900 °C to 1,200 °C with an interval of 50 °C. During the whole testing process, argon was used to prevent the samples from oxidation. The thermal cycle of the hot ductility testing is shown in Figure 1. Firstly, the samples were heated to 1,200 °C and held for 300 s with a heating rate of 10 °C s^{-1} to homogenize the microstructure. Then, the samples were cooled to testing temperatures with a cooling rate of 3 °C s^{-1} and held for 60 s to homogenize the temperature. Finally, the samples were strained until fracture with a strain rate of 10^{-2} s^{-1}. The fractured samples were quenched with high-speed argon flow to protect the fracture surface. In addition, some of the boron containing Fe-36Ni alloy samples were heated to 1,200 °C and held for 300 s. Then, they were cooled to 1,000 °C and held for 60 s. Finally, the samples were strained until the strain is 0.1 and quenched with high-speed argon flow for analyzing the distribution of boron in alloys. The reduction of area (RA%) was used to evaluate the hot ductility of the experimental alloys.

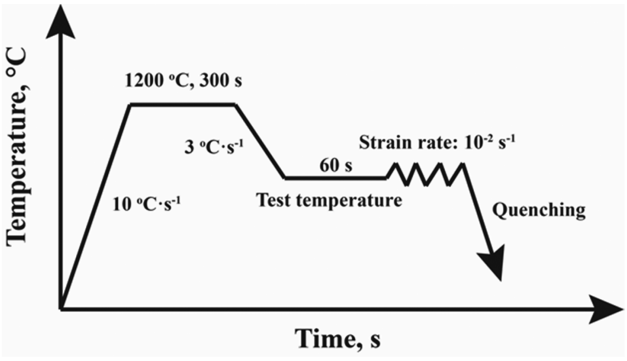

Figure 1: Thermal cycle of the hot ductility test.

Thermo-Calc software with database of TCFE3 was used to calculate the equilibrium precipitation temperature and chemical composition of secondary phase particles in the experimental alloys. The fracture surfaces were observed by use of scanning electron microscopy (SEM, FEI MLA-250). The optical microscopy (OM, Leica DM4M) was used

Table 1: The chemical compositions of the investigated alloys (mass fraction/%).

Alloys	C	Si	Mn	S	Al	N	B	O	Ni	Fe
B0	0.0012	0.17	0.43	0.0031	0.0044	0.0018	–	0.0045	35.97	Bal.
B1	0.0012	0.19	0.43	0.0032	0.0044	0.0019	0.0021	0.0022	35.99	Bal.

to investigate the microstructures and cracks near fracture. The morphology, distribution and chemical composition of precipitates on the carbon replica were analyzed by transmission electron microscopy (TEM, Tecrai G2 F20 S-TWIN) and energy dispersive spectrometer (EDS). Secondary ion mass spectroscopy (SIMS; ION-TOF TOF, SIMS 5) was used to analyze B distribution in the B containing alloys and the scanning area is 300 μm × 300 μm. The samples for OM observation were etched with a mixed solution of 4 g $CuSO_4 \cdot 5H_2O$ + 20 ml deionized H_2O + 20 ml HCl to reveal the microstructures. The carbon extraction replicas used for TEM observation were prepared with plating a carbon film on the sample surface which was etched with 4 g $CuSO_4 \cdot 5H_2O$ + 20 ml deionized H_2O + 20 ml HCl after being mechanically polished. The sample of boron containing alloy used for SIMS analysis was etched with 4 g $CuSO_4 \cdot 5H_2O$ + 20 ml deionized H_2O + 20 ml HCl to reveal grain boundaries for investigating the boron segregation on grain boundaries.

Results and discussion

Hot ductility behavior of experimental alloys

The hot ductility curves of experimental alloys are shown in Figure 2(a). There is a great difference between the RA % values for the experimental alloys at different tested temperatures, indicating that temperature has a significant effect on the variation of hot ductility behaviors. The hot ductility behaviors of both experimental alloys are similar in the temperature region of 900–1,200 °C. The RA% values in the lower single austenite temperature region are below 60 % for both experimental alloys. When the temperature increases above 1,050 °C, the hot ductility improves significantly. Both the RA% values are above 60 % in the temperature region of 1,050–1,200 °C. However, the RA% decreases slightly with increasing temperature from 1,100 °C to 1,200 °C. In the temperature region of 900–1,000 °C, the hot ductility of boron containing alloy B1 is worse than that of boron free alloy B0. In addition, the temperature of brittle fracture of boron containing alloy B1 is 1,000 °C, which is higher than that of boron free alloy B0. There are no obvious differences in the hot ductility behaviors between the tested alloys when the temperature between 1,050 °C and 1,200 °C, indicating that boron has little effect on the hot ductility of experimental alloys at high temperatures.

The strain–stress curves of the investigated alloys at different temperatures are shown in Figure 2(b–c). In the lower temperature region, the flow stress increases to peak stress rapidly after deformation, and then it rapidly decreases to zero which means the fracture occurs. However, the flow stress increases to peak stress slowly with increasing strain and then it decreases until fracture when the temperature is above 1,050 °C. It is obvious that the strain is larger when the temperature is above 1,050 °C compared with that when the temperature is below 1,000 °C, which indicates that the hot ductility in higher temperature region is better than that in lower temperature region. The influencing factors and mechanisms on hot ductility in the temperature region of Zone I (above 1,050 °C) and Zone II (below 1,050 °C) will be discussed.

Analysis of hot ductility behavior in Zone II

The morphologies of fracture surfaces and microstructures near fracture strained at 900 °C are shown in Figure 3. There are no obvious necking phenomena for both experimental alloys. The flat fracture surface indicating that the fracture mode is intergranular. The intergranular fracture occurs when the grain boundary cohesion is weak during the deformation process at high temperatures. In addition, there are some small dimples on intergranular fracture surfaces, indicating that the particles on grain boundaries

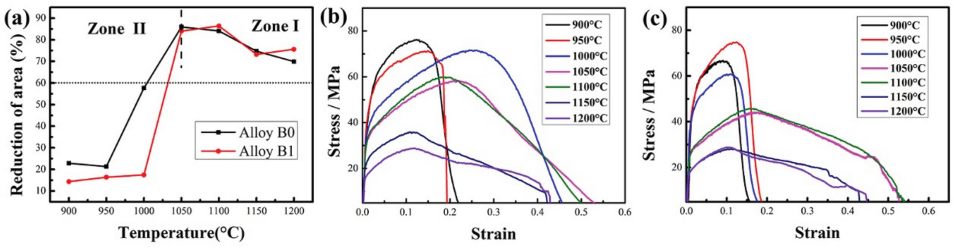

Figure 2: The characteristic curves of the investigated alloys at different test temperatures: (a) reduction of area curves; (b) the stress–strain curves of alloy B0; (c) the stress–strain curves of alloy B1.

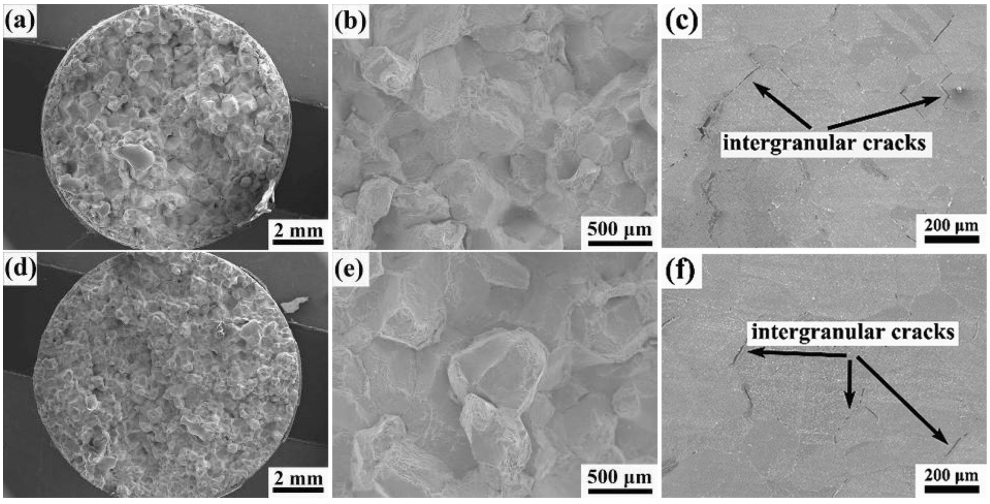

Figure 3: The fractures of the investigated alloys tested at 900 °C in Zone II: (a–c) The macrostructure, microstructure and longitudinal microstructure of the fracture morphology of alloy B0; (d–f) the macrostructure, microstructure and longitudinal microstructure of the fracture morphology of alloy B1.

promoted the nucleation and propagation of micro-cracks during grain boundary sliding, as shown in Figure 3(b) and (e). Moreover, there are many W-type cracks propagating along the vertical direction of tensile stress between grain boundaries, which indicates the occurrence of grain boundaries sliding. All these fracture characteristics show that the fracture mode in the temperature range of 900–1,000 °C is a combination of intergranular decohesion and intergranular micro-void coalescence. The microstructures of the longitudinal sections near the fracture front of alloy B0 and B1 specimens strained at 1,000 °C are shown in Figure 4. There is a part of dynamic recrystallization has happened at 1,000 °C for alloy B0, as shown in Figure 4(a). However, there is no obvious dynamic recrystallization for alloy B1, as shown in Figure 4(b). It indicates that the addition of boron inhibits dynamic recrystallization at 1,000 °C. The occurrence of dynamic recrystallization effectively inhibits the propagation of cracks and hence improves the hot ductility of the investigated alloys.

The effect of secondary phase particles on hot ductility

The equilibrium phase diagrams of the experimental alloys calculated using Thermo-Calc softer package are shown in Figure 5. The oxide inclusions Al_2O_3 form in liquid metal. However, MnS starts to precipitate from austenite when the temperature decreases to 1,350 °C. In boron bearing alloy B1, the BN particle precipitates when the temperature decreases to 1,260 °C, as shown in Figure 5(b).

Alloy B1 is selected to illustrate the effects of secondary phase particles on the hot ductility of the experimental alloy. The morphologies and EDS analysis results of precipitates in the boron bearing alloy B1 was shown in Figure 6, which was investigated using TEM. There are mainly BN, MnS and $(Al,Si)_2O_3$ particles in alloy B1, which is well consistent with the calculation results. In boron bearing alloy B1, the precipitation temperature of MnS and BN are 1,350 °C and 1,260 °C,

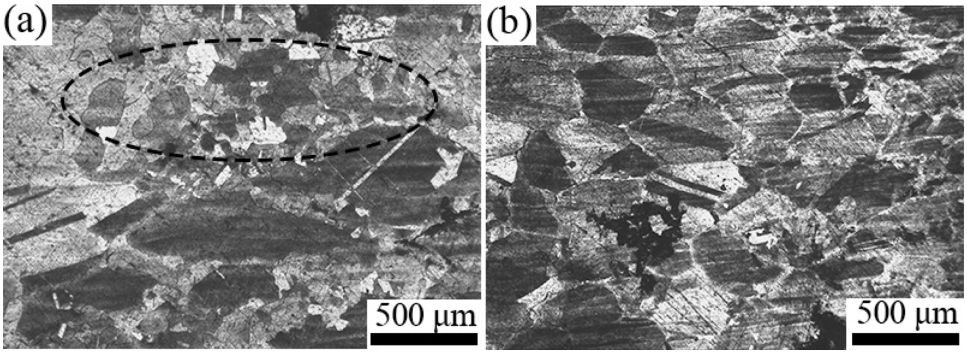

Figure 4: The microstructure of the longitudinal sections near the fracture front of alloy B0 (a) and B1 (b) specimens strained at 1000 °C.

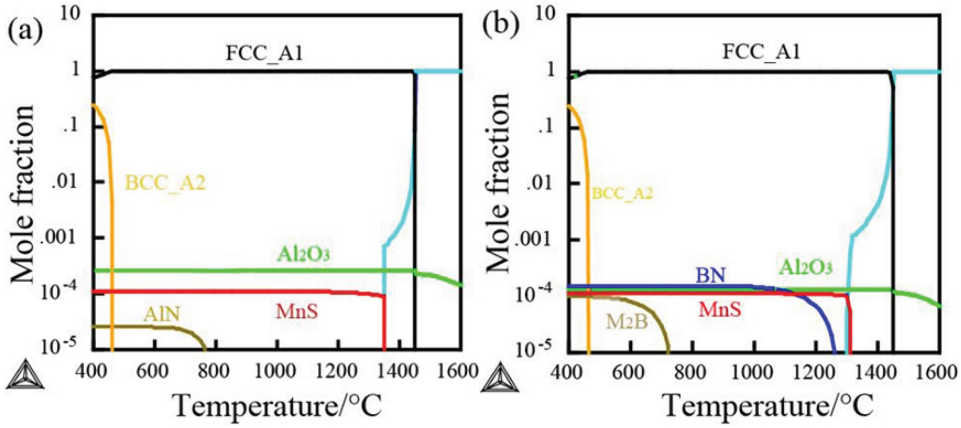

Figure 5: The formation of the secondary phase particles: (a) alloy B0 and (b) alloy B1.

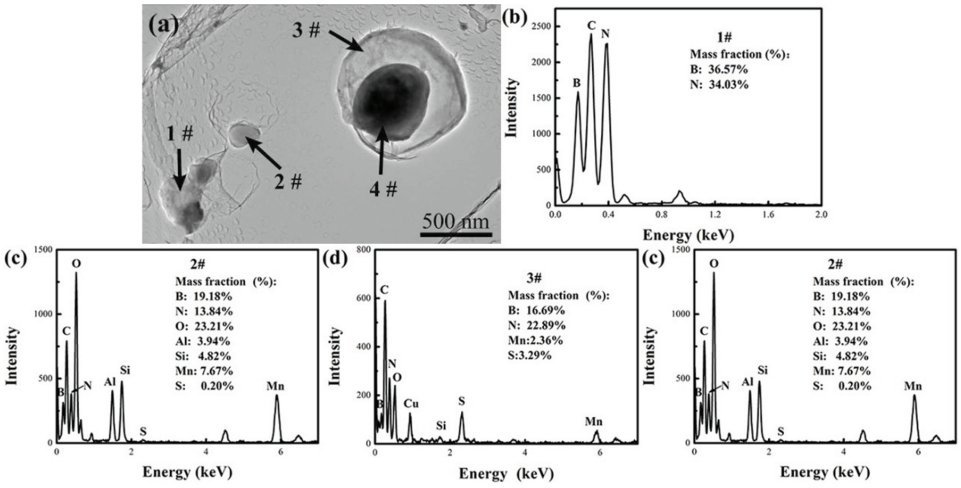

Figure 6: The typical secondary phase particles in alloy B1: (a) The morphology of the secondary phase particles; (b–e) The EDS spectrums of the secondary phase particles denoted by 1–4# in image (a), respectively.

respectively. Since the precipitation temperature of MnS is higher than that of BN, the formation of MnS particles contributes to the heterogeneous precipitation of BN at lower temperatures, resulting in the formation of BN-MnS complex particles. The precipitation of BN on MnS particles, which precipitates on grain boundaries, increases the amount of BN precipitating on grain boundaries, therefore, the grain boundaries cohesion is decreased.

The fine secondary phase particles on grain boundaries, which is obtained from the carbon replica near the fracture front was shown in Figure 7. All these secondary phase particles are BN-MnS, BN-$(Al,Si)_2O_3$ complex particles and MnS particles, indicating there are many fine particles on the grain boundaries in the investigated alloys.

The deformation mechanism of Fe-36Ni alloy in high temperature region is grain boundary sliding [1]. The occurrence of grain boundary sliding promotes the nucleation and propagation of micro-cracks, which deteriorates hot ductility. On the other hand, the occurrence of dynamic recrystallization improves hot ductility of Fe-36Ni alloy significantly. In the experimental alloys, the fine particles on grain boundaries effectively pin the grain boundaries and inhibit the occurrence of dynamic recrystallization. Besides, the fine particles act as nucleus core of micro-cracks during grain boundary sliding and promote cracks nucleation and propagation along grain boundary, resulting in intergranular flat fracture surface and poor hot ductility of the experimental alloys in Zone II. As a consequence, the fine particles on the grain boundaries inhibit the occurrence of dynamic recrystallization

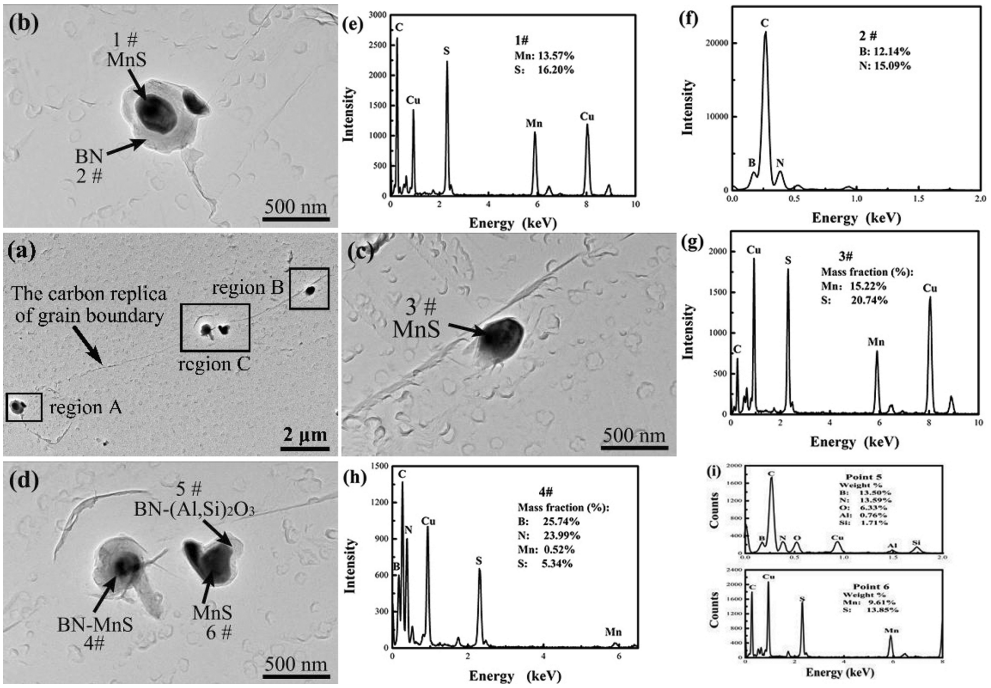

Figure 7: The characteristics of the grain boundaries and secondary phase particles obtained from the carbon replica of alloy B1 specimen tested at 900 °C: (a) the low-magnification image of grain boundaries in the specimen; (b–d) the high-magnification images showing the secondary phase particles on grain boundaries in regions A, B and C, respectively; (e–i) the EDS spectrums of secondary phase particles denoted by 1–6#, respectively.

and promote the nucleation and propagation of intergranular micro-cracks simultaneously, resulting in the poor hot ductility in Zone II.

According to the Thermo-Calc calculation result in Figure 5(b), the amount of BN precipitates increases with decreasing temperature from 1,260 °C to 1,000 °C. Therefore the influence of BN on hot ductility of alloy B1 at 1,000 °C is great, because some BN particles precipitate at grain boundaries which inhibits dynamic recrystallization and decreases grain boundaries cohesion. The hot ductility at low temperatures of 900 °C and 950 °C is bad for the two alloys, because there is no occurrence of dynamic recrystallization. The hot ductility of alloy B1 is worse than that of B0 at low temperature due to the precipitation of BN.

The effect of element segregation to grain boundaries on hot ductility

When the actual Mn:S ratio is higher than the critical Mn:S ratio (Mn:S)c, the free sulfur is prevented to segregate to grain boundaries since the formation of MnS. The formula for calculating the (Mn:S)c is shown in eq. (1). The values of (Mn:S)c are 131.55 and 131.54 for alloys B0 and B1, respectively. Both of these critical values are smaller than the actual values of (Mn:S), which are 138.71 and 134.38 for alloys Bo and B1, respectively. Therefore, the contents of Mn element in the investigated alloys are high enough to combine with all the free S elements, which decreases the detrimental effect of the segregation of sulfur to grain boundaries on the hot ductility. Therefore, the effect of segregation of free sulfur element on hot ductility will not be discussed in the present paper.

The distribution of boron in alloy B1 after the deformation of the experimental alloy to a strain of 0.1 at the temperature of 1,000 °C was investigated by SIMS, as shown in Figure 8. It is obvious that boron segregates to grain boundaries, as shown in Figure 8(b). However, the concentration of nitrogen on grain boundaries is very low, as shown in Figure 8(c). It is indicated that the added boron elements in the investigated alloys mainly segregated to grain boundaries in the form of free atoms during the deformation process at high temperatures.

The large amount of boron atoms segregated to grain boundaries has strong solute drag effect, which retards the occurrence of dynamic recrystallization [15, 16]. In addition, the boron atoms segregated on grain boundaries decreases grain boundary cohesion and

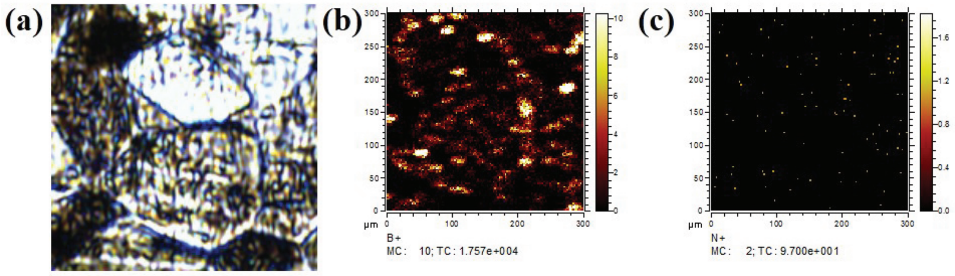

Figure 8: The distribution of the elements in the deformation area of alloy B1 at 1000 °C investigated by the SIMS: (a) the microstructure of the deformation area, (b) the distribution of the B atoms and (c) the distribution of the N atoms.

deteriorate the hot ductility of investigated alloys, which is similar to the effect of sulfur and phosphorus on hot ductility in the other alloys [17]. The segregation of boron atoms and precipitation of BN have a great effect on the hot ductility at 1,000 °C. According to Thermo-Calc calculation result, the amount of BN precipitates increases with decreasing temperature from 1,260 °C to 1,000 °C. The segregation of boron at grain boundaries inhibits dynamic recrystallization effectively at 1,000 °C for alloy B1. Therefore, the hot ductility of boron containing alloy B1 is worse than that of alloy B0 in temperature region of Zone II and the temperature of brittle fracture increases up to 1,000 °C.

Analysis of hot ductility behavior of Zone I

There are no obvious differences between the investigated alloys at high temperatures. Boron has little effect on the hot ductility of Fe-36Ni alloy in the temperature region Zone I. The morphologies of microstructures near fracture surface are shown in Figure 9. All the investigated specimens show obvious necking phenomenon in this tested temperature range, indicating all the specimens experience a large plastic deformation before fracture. When the temperature increases to 1,100 °C, there are many fine grains near fracture surface indicating the occurrence of dynamic recrystallization. The increasing deformation temperature effectively decreases the activation energy of dynamic recrystallization, which promotes the migration of grain boundaries. When the driving force for grain boundaries migration is larger than the pinning effect of fine particles and the solute drag effect of boron segregation on grain boundaries, the dynamic recrystallization occurs [18]. The occurrence of dynamic recrystallization effectively inhibits the propagation of cracks and hence improves the hot ductility of investigated alloys.

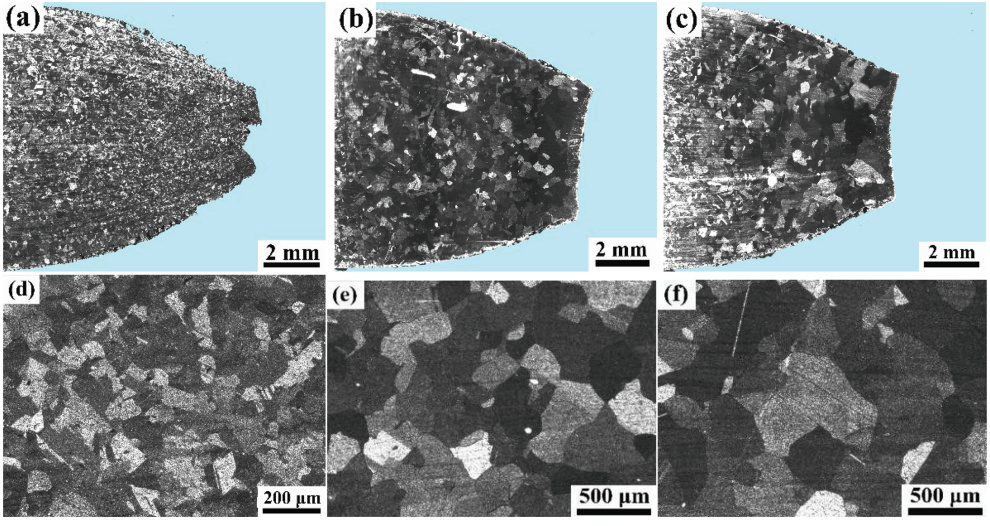

Figure 9: The macrostructure and microstructure of the longitudinal sections near the fracture front of alloy B1 specimens strained at different temperatures: (a, d) 1100 °C; (b, e) 1150 °C; (c, f) 1200 °C.

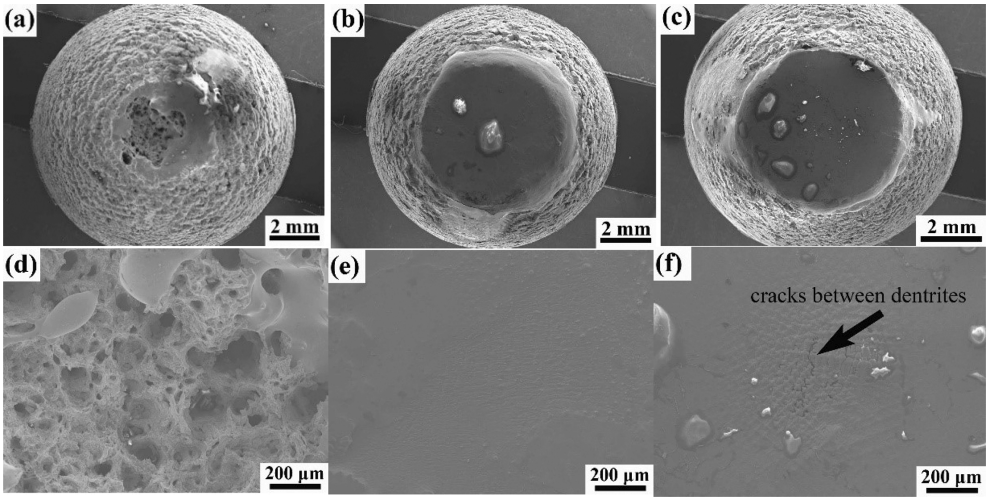

Figure 10: The macrostructure and microstructure of the fracture morphologies of alloy B1 specimens strained at different temperatures: (a, d) 1100 °C; (b, e) 1150 °C; (c, f) 1200 °C.

As shown in Figure 9, the size of the recrystallized grain increases with increasing deformation temperature. Mintz [19] reported that the hot ductility of materials was significantly affected by grain sizes. The stress is prone to concentrate on large grains during the grain boundary sliding, which promotes the nucleation and propagation of cracks. Normally, fine grains hinder the propagation of cracks effectively, which is beneficial for improving hot ductility [12, 20, 21]. There is a little rotation of small size grains during deformation at higher temperatures, which reduces stress concentration on grain boundaries and inhibits the nucleation and propagation of cracks. Besides, fine grains mean there are more trigeminal grain boundaries, which effectively prevent cracks propagation. Therefore, the hot ductility of experimental alloys decreases with increasing temperature at high temperatures.

The morphologies of fracture surface are shown in Figure 10. There are many large and deep dimples on the fracture surface when the temperature is 1,100 °C. However, the fracture surface is flat and melted with the increasing temperature. When the temperature is 1,200 °C, there are many cracks between dendrites, as shown in Figure 10(f). The segregation of impurity elements such as sulfur to dendrite boundaries at high temperature reduces cohesion between dendrites and promotes the nucleation of cracks.

As a consequence, the occurrence of dynamic recrystallization improves the hot ductility of the investigated alloys significantly in the temperature Zone I. However, the coarsening of the dynamic recrystallization grains and the formation of intergranular cracks decreases the hot ductility of the alloys, resulting in gradual decrease of RA% in the temperature Zone I with the increasing temperature.

Conclusions

(1) In temperature region of 900–1,000 °C Zone II, the fine secondary phase particles such as BN and MnS effectively pin the grain boundaries and inhibit the occurrence of dynamic recrystallization, which deteriorates the hot ductility of the investigated alloys. In addition, the fine particles on grain boundaries promote the nucleation and propagation of cracks. Therefore, both of the investigated alloys show poor hot ductility in Zone II.

(2) In the boron bearing alloy B1, the segregation of boron atoms has strong solute drag effect on the grain boundaries, which significantly inhibits the occurrence of dynamic recrystallization. Moreover, the segregation of boron on grain boundaries also impairs the grain boundaries cohesion. Therefore, the hot ductility of alloy B1 is worse than that of alloy B0 in the temperature range of 900–1,000 °C Zone II.

(3) The hot ductility of experimental alloys in temperature region of Zone I is much better than that in Zone II due to the occurrence of dynamic recrystallization. However, the larger grain sizes and initiation of cracks between dendrites deteriorate the hot ductility with increasing temperature.

Acknowledgements: The work is financial supported by China's 13th Plan of Five-year National Key Research and Development Program under Grant No. 2016YFB0300102 and National Nature Science Foundation of China under Grant Nos. 51674020 and 51571019.

References

[1] Y. He, F. Wang, C. Li, Z. Yang, J. Zhang and Y. Li, Mater. Sci. Eng. A., 673(2016) 99–107.
[2] Y. Nakamura, IEEE Trans. Magn., 12(1976) 278–291.
[3] J. Tateno, T. Samukawa and Y. Sodani, ISIJ Int., 56(2016) 1219–1225.
[4] G. Saindrenan, M.T. Simonetta-Perrot, R. Le Gall and R. Louahdi, J. Phys. IV. EDP Sci., 123(2005) 111–115.
[5] S.M. Abbasi, M. Morakabati, R. Mahdavi and A. Momeni, J. Alloys and Comp., 639(2015) 602–610.
[6] L.B. Mostefa, G. Saindrenan, M.P. Solignac and J.P. Colin, Acta Metall. Mater., 39(1992) 3111–3118.
[7] K. Laha, J. Kyono and N. Shinya, Trans. Indian Inst. Met., 63(2010) 437–441.
[8] F. Zarandi and S. Yue, ISIJ Int., 46(2006) 591–598.
[9] S.K. Kim, J.S. Kim and N.J. Kim, Metall. Mater. Trans. A, 33(2002) 701–704.
[10] E. López-Chipres, I. Mejía, C. Maldonado, A. Bedolla-Jacuinde and J.M. Cabrera, Mater. Sci. Eng. A, 460(2007) 464–470.
[11] Y. Zheng, F. Wang, C. Li, J. Cheng and Y. Li, Mater. Sci. Eng. A, 715(2018) 194–204.
[12] K.C. Cho, D.J. Mun, J.Y. Kim, J.K. Park, J.S. Lee and Y.M. Koo, Metall. Mater. Trans. A, 41(2010) 1421–1428.
[13] Y. Yu, W. Chen and H. Zheng, Heat Treatment Met., 39(2014) 118–119.
[14] G.A. Toledo, O. Campo and E. Lainez, Steel Res. Int., 64(1993) 292–299.
[15] X. Wang and X. He, ISIJ Int., 42(2002) S38–S46.
[16] S.I. Kim, S.H. Choi and Y. Lee, Mater. Sci. Eng. A, 406(2005) 125–133.
[17] W. Mo, X. Hu, S. Lu, D. Li and Y. Li, J. Mater. Sci. Technol., 31(2015) 1258–1267.
[18] Y. Fan, M. Wang, H. Zhang, H. Tao, P. Zhao and S. Li, J. Univ. Sci. Technol. Beijing, 35(2013) 607.
[19] B. Mintz, S. Yue and J.J. Jonas, Int. Mater. Rev., 36(1991) 187.
[20] S.H. Song, A.M. Guo, D.D. Shen, Z.X. Yuan, J. Liu and T.D. Xu, Mater. Sci. Eng. A, 360(2003) 96–100.
[21] K.C. Cho, D.J. Mun, M.H. Kang, J.S. Lee and J.K. Park, ISIJ Int., 50(2010) 839–846.